JCIM JOURNAL OF CHEMICAL INFORMATION AND MODELING

Cite This: J. Chem. Inf. Model. XXXX, XXX, XXX−XXX

Article

pubs.acs.org/jcim

Predicting the Affinity of Peptides to Major Histocompatibility Complex Class II by Scoring Molecular Dynamics Simulations

Rodrigo Ochoa,[†] Alessandro Laio,[‡,¶] and Pilar Cossio*[,†,§]

[†]Biophysics of Tropical Diseases, Max Planck Tandem Group, University of Antioquia, 050010 Medellin, Colombia

[‡]International School for Advanced Studies (SISSA), Via Bonomea 265, 34136 Trieste, Italy

[¶]The Abdus Salam International Centre for Theoretical Physics (ICTP), Strada Costiera 11, 34151 Trieste, Italy

[§]Department of Theoretical Biophysics, Max Planck Institute of Biophysics, 60438 Frankfurt am Main, Germany

Supporting Information

ABSTRACT: Predicting the binding affinity of peptides able to interact with major histocompatibility complex (MHC) molecules is a priority for researchers working in the identification of novel vaccines candidates. Most available approaches are based on the analysis of the sequence of peptides of known experimental affinity. However, for MHC class II receptors, these approaches are not very accurate, due to the intrinsic flexibility of the complex. To overcome these limitations, we propose to estimate the binding affinity of peptides bound to an MHC class II by averaging the score of the configurations from finite-temperature molecular dynamics simulations. The score is estimated for 18 different scoring functions, and we explored the optimal manner for combining them. To test the predictions, we considered eight peptides of known binding affinity. We found that six scoring functions correlate with the experimental ranking of the peptides significantly better than the others. We then assessed a set of techniques for combining the scoring functions by linear regression and logistic regression. We obtained a maximum accuracy of 82% for the predicted sign of the binding affinity using a logistic regression with optimized weights. These results are potentially useful to improve the reliability of *in silico* protocols to design high-affinity binding peptides for MHC class II receptors.

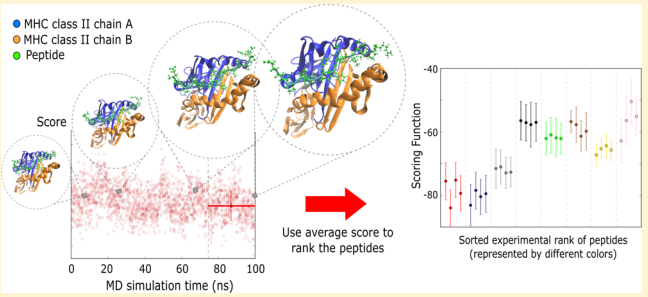

INTRODUCTION

The major histocompatibility complex (MHC) class II molecules are key receptors involved in adaptive immunity. MHC class II molecules respond against extracellular proteins,[1] in particular, small peptides to which they bind to activate the immune system. Due to their role in the control of infections caused by external pathogens,[2] understanding the MHC class II binding mechanisms, and predicting the binding affinity to peptides, has become a priority.

The molecular mechanisms by which MHC class II recognizes peptides has been investigated in detail.[3] The peptides bind to a groove exposed on the external regions $\alpha 1$ and $\beta 1$ of the MHC class II receptor, which is characterized by two α-helical walls and a β-sheet.[3,4] The binding peptides can have a length between 9 and 20 amino acids.[4] However, the complex is mainly stabilized by the interactions of 9 amino acids, which are localized in four key pockets: P1, P4, P6 and P9 (see Figure S1). The pockets are distributed between the $\alpha 1$ and $\beta 1$ regions, with the latter containing multiple polymorphisms, associated with different MHC class II alleles.[5] The flanking regions of the peptide, as well as the amino acids that do not interact with the key pockets, are crucial to facilitate the interaction with T-cell receptors (TCRs) after migration of the peptide−MHC complex to the surface of antigen-presenting cells.[6]

The identification of peptides that potentially trigger immune responses against invading pathogens relies, in part, on the binding affinity between the peptide and the MHC class II receptor.[7] If the binding affinity is high, the peptide has a greater potential to trigger an immune response. This hypothesis has been associated with antigenicity and immunogenicity properties of the source peptides.[8] However, there are other factors that could affect the immunological response of the peptides, such as the complementary of the peptide−MHC complex with TCR loops, the stability of the interaction between the peptide and the MHC class II, and the facilitation of the editing process made by additional proteins.[9,10] With these premises, the area of immunoinformatics has developed an extensive set of bioinformatics tools (mainly sequence-based strategies) for predicting the affinity between a peptide and MHC class I or class II molecules.[11] These bioinformatics pipelines should detect if novel peptides derived from pathogen proteins can be used as vaccine candidates, or can help other antigens trigger the immune

Received: May 13, 2019
Published: July 10, 2019

DOI: 10.1021/acs.jcim.9b00403
J. Chem. Inf. Model. XXXX, XXX, XXX−XXX

molecular machinery.[12] These methods are widely used by the community. However, the MHC class II molecules are flexible, and the binding-affinity prediction for novel sequences is a difficult task.[13] Moreover, these approaches require extensive training sets of peptides of different sizes assayed under standardized competitive binding experiments, which might not be available.

An alternative and a complement to the bioinformatics-based approaches are structure and dynamic-based strategies. This is made possible by the availability of MHC class II structures in complex with peptides derived from pathogens, or involved in autoimmune diseases.[14,15] The inclusion of structural information is crucial to explore relevant molecular conformations of the peptide−MHC complex, and therefore, key to understand its dynamic behavior.[16] Methodologies using regular or enhanced sampling approaches with molecular dynamics (MD) simulations have been applied to predict the free energy of binding between pathogen-derived peptides and MHC molecules.[17,18] Concerns about these strategies include the required computational time, and the intrinsic errors of the binding prediction.[19] One way to solve these issues is through integrative approaches, which in many cases are able to predict accurately and efficiently the experimental binding data.[20] These strategies may provide a rational way to modify the amino acid sequence[21] by improving the affinity of the peptide−MHC complex.

A possible approach is to use MD to generate a realistic ensemble of configurations of the complex, and then score it with a scoring function for predicting the binding affinity.[22−25] These combined approaches have been designed to make virtual screening more reliable, accurate and fast,[26,27] for discriminating between binders and nonbinders, and between binding poses of the same molecules.[28] Although these methods are less accurate than calculating the binding free energy by molecular dynamics, they provide a viable compromise between predictive power and computational efficiency.[29,30] A crucial step in these calculations is the selection of the scoring functions, which can be knowledge-based, physics-based, or a hybrid composite function.[31]

The purpose of this work is to refine this approach, with the specific target of predicting the experimental binding affinity to MHC class II. We considered a set of eight peptides of known binding affinity. We modeled the complexes formed by the peptides with an MHC class II molecule by accurate explicit-solvent MD simulations, and then scored the conformations from these simulations using 18 scoring functions. We assessed the performance in predicting the experimental rank of the peptides. Six scoring functions produced good predictions. We then combined these scoring functions using linear regression and logistic regression models. We show that combining different scoring functions produced better results than any individual score, and the best results are found using a logistic regression model.

METHODS

MHC Class II Binding Data Set and Structure Selection. A data set containing 44 541 measured affinities covering 26 MHC class II alleles was chosen.[32] The set includes binding data of different HLA-DR, DP, and DQ receptors obtained from experiments under equal conditions for all the peptides. This information is part of the training data implemented by prediction tools available at the IEDB portal.[33] Oligopeptides of different sizes are included, but with a major proportion of 15-mer peptides bound to HLA-DR receptors (∼95%).

Additionally, we looked in the Protein Data Bank (PDB)[34] for protein structures of HLA-DR receptors in complex with peptides. We focused on structural complexes that had available binding affinities from the chosen data set. Only a structure of the HLA-DRB1*15:01 allele cocrystallized with a 15-mer peptide derived from the myelin basic protein (MBP)[35] met the selection criteria (PDB id: 1BX2). This structure was selected as the template to model different peptides from the data set. The structure was subjected to reconstruction of missing side chains using Scwrl4.[36]

Selection of the Peptides. The selected structure (1BX2) is in complex with the peptide of sequence ENPVVHF-FKNIVTPR. On the basis of this template, we selected peptides sharing identical amino acids in the 9-mer core region that interact with the HLA-DR pockets. Two methodologies were used to predict the 9-mer core part of all the 15-mer peptides available in the data set. One method is based on a position-specific scoring matrix previously created for the HLA-DRB1*15:01 allele using multiple sequence alignments of known substrates.[37] Specifically, the sequences were analyzed using windows of nine amino acids, starting from different initial positions, and each fragment was scored and summed to obtain a ranked list for the position of the most probable core region. The fragment with the highest score was selected. The second method implements the NetMHCIIpan-3.1 tool, which has been designed for the quantitative prediction of peptide binding to MHC class II molecules, and also for the prediction of the 9-mer core regions of any peptide sequence.[38]

We filtered the peptides with identical core regions predicted by both methods, and selected the peptides with the highest scores in comparison to those calculated for the reference sequence. We also filtered the peptides by the maximum number of amino acids shared within the core regions of the crystal, mainly sequences with identical amino acids interacting in positions P1, P4, P6, and P9. This analysis was done to avoid misalignment of the core region, and obtain reliable starting models for the peptide−MHC class II complexes. Moreover, we selected peptides with experimental affinities differing in a wide range of IC50 values. The final list of chosen peptides for the posterior modeling and evaluation of the sampling/scoring approach are shown in the Results section, Table 1.

Modeling of Peptides Bound to MHC Class II Receptor. We selected as the template, over which to model the seven selected peptides, the peptide-bound MHC class II PDB structure (1BX2).[35] The modeling protocol was an iterative single-point mutation approach using the Rosetta fixbb package,[39] which was previously compared to other available mutation protocols.[40] Each amino acid position was mutated using Rosetta fixbb with a subsequent relaxing phase of the amino acid side chains with fixed backbone. Some peptides had additional amino acids at the amino or carboxi terminal positions of the core region. These were modeled using the Rosetta Remodel package from RosettaCommons.[41] The new amino acid, as well as the amino acids next to it were subjected to the prediction of rotamers with relaxation of the side chains.

Molecular Dynamics Simulations. Each protein−peptide complex from the benchmark was subjected to 100 ns of MD simulations with previous minimization and NVT/NPT

DOI: 10.1021/acs.jcim.9b00403
J. Chem. Inf. Model. XXXX, XXX, XXX−XXX

equilibration phases. GROMACS v5.1[42] was used to perform the MD simulations. The Amber99SB-ILDN protein force-field[43] and TIP3P water model[44] were used. The protein was solvated in a cubic box of water with periodic boundaries at a distance of at least 8 Å from any atom of the protein. After solvation, counterions of Na^+ and Cl^- were included in the solvent to make the box neutral. The electrostatic interactions were calculated using the Particle Mesh Ewald (PME) method with 1.0 nm short-range electrostatic and van der Waals cutoffs.[45] The equations of motion were solved with the leapfrog integrator[46] using a time step of 2 fs.

The simulations were performed at a temperature of 350 K to allow a fast exploration of the conformational space. We used a modified Berendsen thermostat[47] and a Parrinello–Rahman barostat.[48] To maintain the system stable at this temperature, all the receptor atoms located in a distance greater than 12 Å from any peptide atom were restrained. The atoms from the receptor located in a distance lower than the threshold remained flexible, as well as the peptide. The convergence of the simulations was monitored by computing the number of hydrogen bonds between the peptide and protein, the number of heavy atom contacts,[49] the all-atom root mean-square deviation (RMSD) of the peptide and the root mean-square fluctuation of both the protein and the peptide.

Scoring Functions. A set of 18 different scoring functions was used to score the conformations from the MD trajectories. We selected the following: ROSETTA,[50] PISA,[51] FIRE-DOCK,[52] ZRANK,[53] BACH,[54−56] BMF,[57] BLUUES,[58] a method combining the results of BMF and BLUUES (BMF-BLUUES), HADDOCK,[59] VINA,[60] DFIRE,[61] GOAP,[62] the combination of the results from DFIRE and GOAP (DFIRE-GOAP), IRAD,[63] ODA,[64] PROPNSTS,[65] SIPPER,[65] and PRODIGY.[66] Details for each scoring function are provided in the Supporting Information.

Most of the scoring functions are statistical and knowledge-based potentials used for protein−protein and protein−ligand docking. However, semiempirical approaches are also included. The scores were calculated using the complete protein−peptide complex conformations. We used the last quarter of the MD trajectories to calculate the average score and the standard deviation for each complex. Specifically, we used the last 25 ns for the analysis, and we took snapshots of the system every 50 ps, resulting in 500 structures for each peptide−MHC class II complex. In the Supporting Information we also provide the results using the last half of the trajectory. A general schema of the protocol is provided in Figure 1.

Block and Spearman Correlation Analysis. A block analysis approach was applied to estimate the statistical reliability of the scores. Specifically, the last quarter of the trajectory was split into four blocks of equal length, and the mean and standard deviation of the scores were calculated in each block. We then selected at random one of the four blocks for each peptide, and computed the Spearman correlation using only that block. We repeated this procedure 2000 times, obtaining in this manner a probability distribution of the Spearman correlation. The cumulative and the average of each correlation distribution were used to rank and select the best scoring functions for further analysis (see Results).

Pair Analysis and Consensus Strategies. For each possible pair of peptides, we evaluated if the sign of the difference between the predicted scores are in agreement with the experimental activity difference ($\Delta\Delta G$). On this basis, we

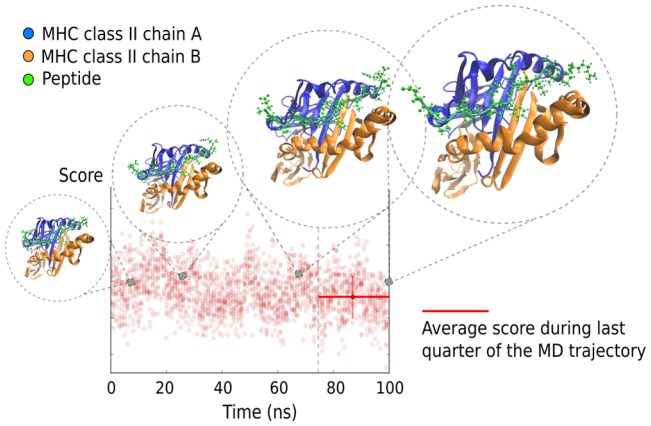

Figure 1. Schematic representation of the sampling and scoring strategy used to analyze the conformations from the finite-temperature MD trajectories between the MHC class II and each peptide. The converged last quarter of the trajectory is used to calculate the average and standard deviation of the score.

checked separately for each scoring function, and in a consensus framework (see below), if a peptide compared to another increases or decreases the activity as a dichotomous response.

For the consensus strategies, we verified if the prediction agrees with the sign of the experimental $\Delta\Delta G$ between peptide A and peptide B ($\Delta\Delta G_{AB}$).

The first consensus strategy is based on a linear regression model. In this case, the independent variables are the differences of the scores for each pair of peptides, and the response variable is the predicted $\Delta\Delta G$. The prediction is correct if the sign of the predicted $\Delta\Delta G$ is equal to the sign of the experimental $\Delta\Delta G$. To cross-validate the model, we trained and tested it using a leave-out-one strategy. This consisted of removing one peptide from the training set, and building the test group with the possible pairs made between the removed peptide and all the other peptides. The process was repeated for all the available peptides. To assess the robustness of the model, the final performance was averaged between all the sets generated with the leave-one-out strategy.

The second consensus strategy is logistic regression of the sign of the $\Delta\Delta G_{AB}$ for each pair of peptides A and B. To represent the data, we generated bitstrings (namely vectors containing ones and zeros), where at each position a value of 0 or 1 was assigned according to the sign of $S_k^A - S_k^B$ for each scoring function k. S_k^A is the value of the average score for peptide A, and S_k^B for peptide B. The bitstrings are given by

$$\begin{cases} 1, & sign(S_k^A - S_k^B) = sign(\Delta\Delta G_{AB}) \\ 0, & otherwise \end{cases} \quad (1)$$

An advantage of these methods is the possibility to assign different weights for each scoring function. The training and validation strategy is the same as applied to the linear regression model (i.e., the leave-one-out approach). The fitting and validation of both the linear and logistic regression models were implemented with the scikit-learn package.[67]

After running the two consensus strategies, we selected the one with the highest performance to evaluate the errors using the bootstrapping approach previously explained. We ran the consensus strategy 2000 times using random blocks of the

DOI: 10.1021/acs.jcim.9b00403
J. Chem. Inf. Model. XXXX, XXX, XXX−XXX

Table 1. List of Selected Peptides with Core Predictions Similar to the Template Peptide (Bold Sequence)[a]

Full peptide	Predicted core	M1[b]	M2[c]	AA core[d]	kAA core[e]	IC50 [nM]
ENPVVHFFKNIVTPR	**VHFFKNIVT**	17.68	0.61	9	4	3.73
GINITNFRAILTAFS	ITNFRAILT	11.25	0.63	3	2	9.89
RPGVSKKFLSLLTSS	SKKFLSLLT	8.29	0.64	2	2	19.96
SMVGLFSNNPHDLPL	VGLFSNNPH	13.05	0.55	3	3	113.96
EICEVVLAKSPDTTC	VVLAKSPDT	2.01	0.79	3	2	284.65
SLLVAPMPTASTAQI	VAPMPTAST	5.34	0.56	2	2	537.75
AFALVLLFCALASSC	VLLFCALAS	13.09	0.42	2	2	1489.02
VVLGLATSPTAEGGK	VLGLATSPT	8.97	0.63	2	2	8320.10

[a]The prediction scores per method (M1 and M2), the number of identical amino acids in the core region (AA core and kAA core), and the corresponding IC50 values are shown. [b]Method to predict the core region using the position-specific scoring matrix. [c]Method to predict the core region using the NetMHCIIpan-3.1 tool. [d]Identical amino acids in the core region to the template. [e]Identical amino acids in the core region interacting with key pocket regions of the template.

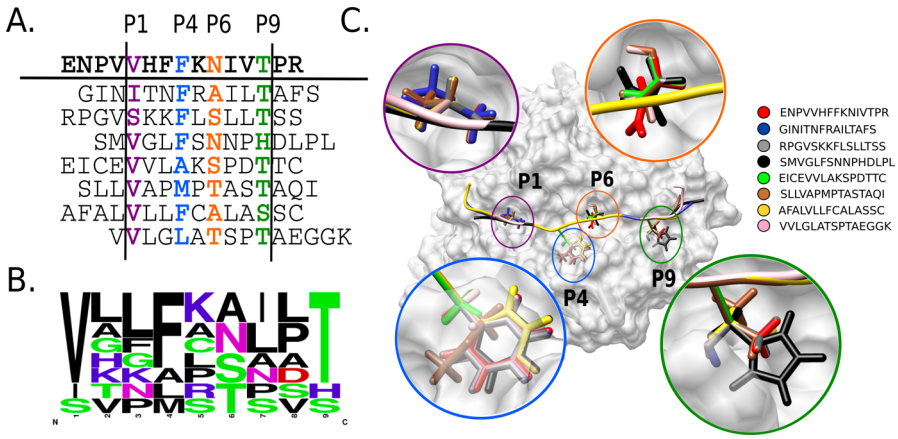

Figure 2. Peptides bound to the MHC class II interface modeled using as template structure PDB: 1BX2. (A) Set of selected peptides. The template peptide is shown in bold. The alignment of the peptide sequences in the core region is shown. The amino acids that interact with the protein pockets are colored in purple (P1), blue (P4), orange (P6), and green (P9). (B) Logo of the predicted core fragments, with amino acid properties colored in purple (positive charged), red (negative charged), green (small), fucsia (asparagine), and black (aliphatic). (C) Initial conformations of the modeled peptides bound to the MHC class II interface.

mean scores. The final accuracy was averaged across all replica, and compared to the previous consensus results.

RESULTS

We modeled a set of peptides bound to a MHC class II receptor which had available experimental binding data. The models were generated using as template a crystal of a HLA-DRB1*15:01 protein in complex with a 15-mer peptide (see Methods). The conformations were sampled using all-atom molecular dynamics. The last quarter of the trajectories were scored, using different programs, and the correlations against experimental activities were calculated. With this approach, we use protein−peptide structural and dynamical information, as well as consensus approaches for predicting the experimental data.

Modeling and Simulation of the Bound Peptides. We selected eight peptides (Table 1) bound to the MHC class II receptor following the selection criteria described in the Methods section. The binding affinity of these peptides has been evaluated experimentally under the same conditions. A crystal structure for one of these peptides bound to the receptor is reported in the PDB (PDB id: 1BX2). This crystal was used as a template to model the other structures. To align and model the peptides to the target structure, we implemented two programs (see Methods) that predicted the core regions of the peptides. The prediction of the core region was consistent in both methods, revealing the location of the amino acids that interact with key pockets from the protein receptor. All the selected peptides contain some amino acids on the predicted core region that are conserved on the peptide template. The experimental IC50 values vary in a range from ∼3 to ∼8300 nM (Table 1)

Despite that the selected peptides belong to different protein sources, crucial amino acids are conserved in the core region. This allows us to use a modeling approach based on the template structure, which maintains the peptide backbone fixed and a polyproline-II like characteristic conformation.[68] The sequence alignment of the modeled peptides and their initial structural models are available in Figure 2. After generating an initial model for the peptides, we performed 100 ns MD simulations at 350 K to sample the finite-temperature conformational ensemble. The computational time required to run the analysis was approximately 72 h per protein−peptide complex in a 32-core CPU machine with GPU acceleration. The models after the MD simulations are shown in Figure S2. We calculated different observables (e.g., number of hydrogen bonds, RMSD) over the conformations from the MD simulation. We found that despite the intrinsic flexibility of the peptides, the complexes remain stable, and part of the interactions are made with key residues of the MHC class II β1 region such as Arg11, Phe24, Ala72, and Val84, which are classified as polymorphisms among the reported alleles. A

DOI: 10.1021/acs.jcim.9b00403
J. Chem. Inf. Model. XXXX, XXX, XXX−XXX

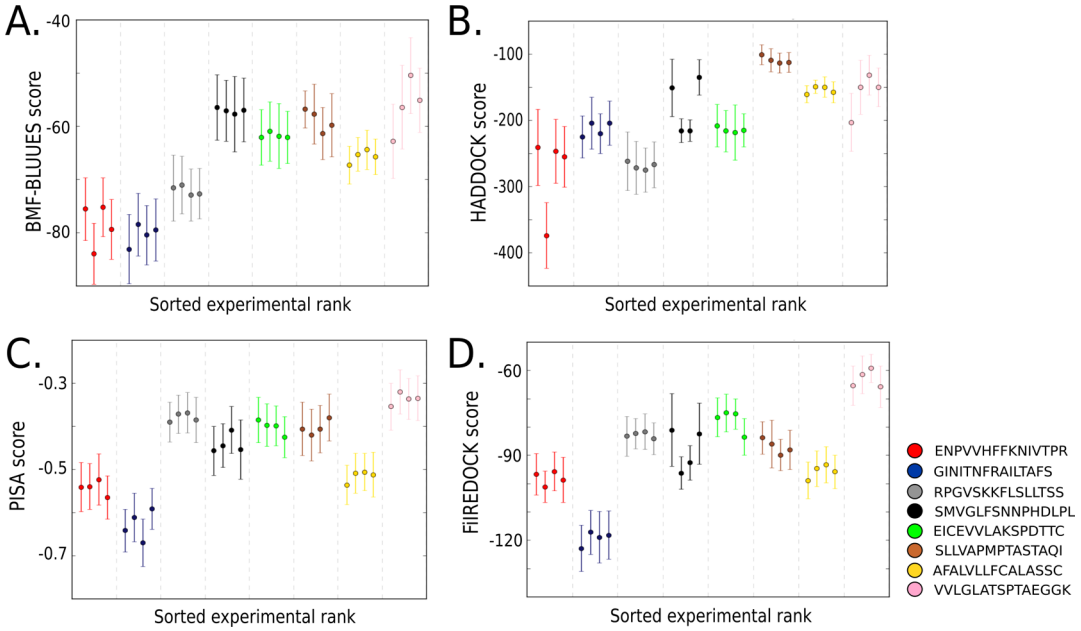

Figure 3. Estimated affinity for four scoring functions: BMF-BLUUES (A), HADDOCK (B), PISA (C), and FIREDOCK (D) over the last quarter of the MD trajectory divided in 4 blocks. The peptides are sorted from highest activity (left) to lowest (right). Each peptide is labeled by a color, and the blocks are represented by the average score and standard deviation.

summary of these observables is available in the Supporting Information (Figures S3 and S4). An additional indicator of the stability of the peptides is the average number of contacts (Figure S5 for peptides SLLVAPMPTASTAQI and VVLGLATSPTAEGGK). For the majority of peptides these observables are stable.

Scoring the MD Conformations. Eighteen different scoring functions for protein−protein interactions were used to calculate scores over the conformations from the last quarter of each MD trajectory. After running the block analysis (see Methods), we find that depending on the peptide and on the scoring function, the average scores can slightly deviate between blocks, but in general, they maintain a stable behavior (see Figures S6 and S7). However, some scoring functions are more variable than others, which could affect the discrimination between binders. In Figure 3, we show the correlation of four different scoring functions to the experimental data. The average-score for the peptides is ploted as a function of the sorted experimental affinity. Thus, the peptide with the higher affinity is located in the left of the plot, and the one with the lowest affinity in the right.

The scoring functions HADDOCK, PISA, BLUUES, BMF-BLUEES, VINA, FIREDOCK, and DFIRE-GOAP had correlations above 0.5 with the experimental data. However, many of the scoring functions were not able to predict accurately the experimental rank of the peptides. This could be associated with the nature of each scoring function. We note that combining sampling with scoring methods improves the robustness of the prediction by avoiding outliers due to the use of a single conformation, which might not be representative of the equilibrium ensemble.

Spearman Correlation Statistical Analysis. A statistical analysis of Spearman correlation was used to compare the predicted ranks to the experimental peptide ranks. For each scoring function, we used the bootstrapping schema with 2000 replica (see Methods) to calculate the distribution of the Spearman correlation. This strategy was motivated because of the variability between the blocks (see Figure 3), and it was developed to obtain a robust statistical measure of the peptide rankings. The cumulative probabilities obtained after bootstrapping for some of the scoring functions are shown in Figure 4.

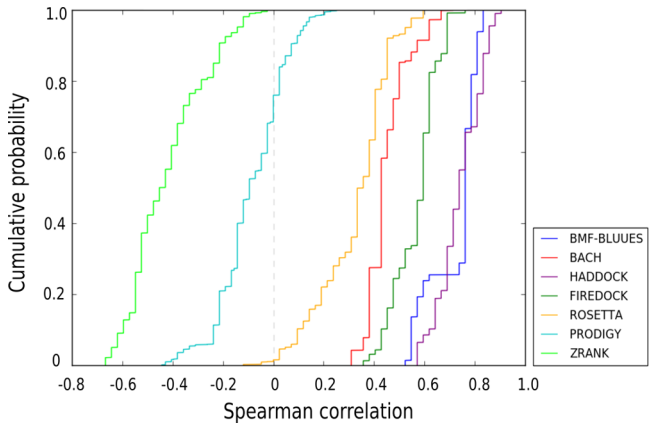

Figure 4. Cumulative probability distributions of Spearman correlations calculated after bootstrapping with 2000 replica for the scoring functions BACH, HADDOCK, FIREDOCK, ROSETTA, PRODIGY, ZRANK, and the combination BMF-BLUUES.

The results show that there are some scoring functions that predict well the experimental rankings. Scoring functions HADDOCK and BMF-BLUUES are the ones with better performances (correlations above 0.7). However, in other cases, some scoring functions, such as BACH, had an average performance (∼0.4). The statistical potentials ZRANK and PRODIGY had poor performances with negative correlations. The cumulative distributions for all the scoring functions are shown in Figure S8, and a final list of the average scoring correlations for the 18 scoring functions is available in Table 2.

DOI: 10.1021/acs.jcim.9b00403
J. Chem. Inf. Model. XXXX, XXX, XXX−XXX

Table 2. Average Spearman Correlation for Each Scoring Function Obtained from the Boostrapping Analysis Using the Last Quarter and Last Half of the Trajectory at 350 K[a]

Scoring function	Correlation last quarter, 350 K	Correlation last half, 350 K
HADDOCK	0.739	0.690
BMF-BLUUES	0.726	0.664
BLUUES	0.685	0.678
DFIRE-GOAP	0.645	0.648
PISA	0.581	0.566
VINA	0.577	0.465
FIREDOCK	0.571	0.569
GOAP	0.499	0.526
BACH	0.451	0.531
DFIRE	0.442	0.430
ODA	0.408	0.434
ROSETTA	0.325	0.406
BMF	0.314	0.349
PRODIGY	−0.085	−0.179
PROPNSTS	−0.174	−0.188
IRAD	−0.211	−0.119
SIPPER	−0.303	−0.303
ZRANK	−0.427	−0.290

[a]The results are sorted in descending order based on the correlations of the last quarter of the trajectory at 350 K.

The Spearman correlation distributions for all the scoring functions was also calculated using half of the MD trajectory (see Figure S9 and Table 2). In general, the performance for the best scoring functions was similar but slightly poorer than the one obtained using the last quarter of the MD.

Ranking Using Consensus Approaches. We now assess different consensus approaches that can improve the predictability obtained by a single scoring function. Six scoring functions with an average Spearman correlation higher than 0.5 were selected to evaluate various consensus approaches. From the list described in Table 2, we selected HADDOCK, BMF-BLUUES, DFIRE-GOAP, PISA, VINA, and FIREDOCK. We use these scoring functions for predicting the sign of the difference in experimental affinity between pair of peptides (see Methods). Specifically, we tested the scoring functions on eight different subsets, where each subset contains all the possible peptide pairs made by one of the selected peptides with respect to all the others. In Table 3, we show the performance to predict the experimental sign of the binding affinity for each scoring function for each subset. The last row shows the averaged performance of each scoring function among the eight subsets. We found that HADDOCK, BMF-BLUUES, and DFIRE-GOAP are the ones with higher accuracy (∼78−80%).

Subsequently, we evaluate the two proposed consensus approaches (see Methods). The performances on the same eight subsets of pairs of peptides are available in Table 4. The first consensus strategy that we used was a linear regression model, that assigns different weights to each scoring function. To avoid evaluating the performance on a set used for training the model, we implemented the leave-one-out strategy (see Methods). In general, the linear regression had the worst results, with an average performance of ∼59% (Table 4). The low performance can be explained by the highly colinearity of the predicted score differences (see Table S1), the presence of outliers or, possibly, fitting-optimization issues derived from the calculation of the parameters. For this model, we also calculated the Spearman correlation coefficient to the $\Delta\Delta G$. The results per subset are included in the Supporting Information Table S3. We note that because this model is only trained to predict the sign, and not the exact score, for some peptides its performance is not ideal.

Table 4. Performance of Consensus Strategies by Regression Models (Linear and Logistic) in the Prediction of the $\Delta\Delta G$ Sign[a]

Peptide for testing	Linear regression model	Logistic regression model
ENPVVHFFKNIVTPR	57.14	92.86
GINITNFRAILTAFS	85.71	100.00
RPGVSKKFLSLLTSS	42.86	92.86
SMVGLFSNNPHDLPL	57.14	57.14
EICEVVLAKSPDTTC	42.86	85.71
SLLVAPMPTASTAQI	85.71	85.71
AFALVLLFCALASSC	42.86	57.14
VVLGLATSPTAEGGK	57.14	85.71
Average	58.93	82.14

[a]We generated subsets of peptides-pairs, where each row corresponds to the subset of pairs made by the peptide with all the others. The performance is shown for each subset, and the average for each consensus method is shown in the last row.

Lastly, we considered the consensus approach to predict the rankings between pairs with a logistic regression model (see Methods). We used the same leave-one-out validation protocol. We found the highest average performance in our study: 82.14% (Table 4). An advantage of this model is the assignment of weights that depend only on the combination of

Table 3. Performance of Each Scoring Function (S1 to S6) in the Prediction of the Experimental $\Delta\Delta G$ Sign[a]

Peptide for testing	FIREDOCK	HADDOCK	PISA	BMF-BLUUES	DFIRE-GOAP	VINA
ENPVVHFFKNIVTPR	85.71	100.00	85.71	85.71	100.00	71.43
GINITNFRAILTAFS	85.71	71.43	85.71	85.71	85.71	85.71
RPGVSKKFLSLLTSS	57.14	85.71	42.86	100.00	85.71	85.71
SMVGLFSNNPHDLPL	71.43	85.71	71.43	57.14	57.14	85.71
EICEVVLAKSPDTTC	71.43	71.43	57.14	71.43	71.43	71.43
SLLVAPMPTASTAQI	57.14	71.43	57.14	71.43	71.43	71.43
AFALVLLFCALASSC	42.86	71.43	42.86	57.14	71.43	28.57
VVLGLATSPTAEGGK	100.00	71.43	100.00	100.00	100.00	100.00
Average	71.43	78.57	67.86	78.57	80.36	75.00

[a]We generated subsets of peptides-pairs, where each row corresponds to the subset of pairs made by the peptide with all the others. The performance is shown for each subset, and the average for each scoring function is shown in the last row.

DOI: 10.1021/acs.jcim.9b00403
J. Chem. Inf. Model. XXXX, XXX, XXX−XXX

rankings and not on the predicted numerical values (see Table S2). To statistically validate the logistic regression performance, we calculated the consensus results using the bootstrapping strategy previously explained (see Methods). This is crucial in order to include the variability of each scoring function in different parts of the trajectory. We found an average accuracy of 75.69% (Table 5), which is a high correlation since it uses only blocks of the trajectory of 100 ns that are ∼7% of the total.

Table 5. Pairwise Analysis of the Performance in Predicting the Experimental ΔΔ*G* Sign (Average and Standard Deviation) Using the Logistic Regression Model with Bootstrapping (BS) after 2000 Replica

Peptide for testing	Logistic with BS[a]	Standard deviation
ENPVVHFFKNIVTPR	88.86	8.00
GINITNFRAILTAFS	84.80	10.92
RPGVSKKFLSLLTSS	75.51	16.81
SMVGLFSNNPHDLPL	62.95	9.10
EICEVVLAKSPDTTC	76.42	8.25
SLLVAPMPTASTAQI	79.20	6.57
AFALVLLFCALASSC	51.51	6.79
VVLGLATSPTAEGGK	86.30	12.09
Average	75.69	

[a]Logistic regression with bootstrapping.

DISCUSSION

We found that combining molecular dynamics sampling with classical scoring functions is a suitable computational strategy to obtain significant correlations (>0.7) with experimental binding-data of MHC class II complexes. This method opens the possibility to implement a structure and dynamic-based approach for ranking novel peptides, which do not have homologous counterparts in existing databases. The approach does not require the use of machine learning methods to predict binding affinities that are training-set dependent. We envision the strategy useful for design protocols that use iterative single-point mutations, which novel peptides can be further evaluated as subunit vaccine candidates,[69] or as modulators of autoimmune diseases.[70]

An initial crucial step is the modeling of the starting configuration of the peptide bound to MHC class II. We used a crystal structure as a template, and a bioinformatics analysis to predict the amino acid positions of the peptide in the binding pocket. To facilitate the peptide modeling, we selected an MHC class II structure bound to a peptide with reported bioactivity data.[32] However, we note that it is possible to model the peptides using other reference structures. The first step of our protocol is stabilizing the complex by using a long MD simulation. Therefore, our approach can be applied also if the structure of the complex is only approximately known. We used an iterative single mutation approach to model the side chains, motivated by a previous assessment of various protocols to mutate amino acids in peptide chains.[40] A limitation during the initial modeling is not including the entropic contributions required to potentially change the peptide conformation. However, this is overcome by using equilibrium distributions from molecular dynamics simulations.

For the MHC class II, the identification of the core region is crucial to know the most probable conformation of the peptides bound to the MHC class II interface. Most of the machine learning methods[11,38] include the prediction of which amino acids can interact with key pockets in the core. For our assessment, we prioritized peptides having at least a few amino acids identical to the target crystal to avoid wrong initial peptide-binding configurations.

Moreover, we found that using MD simulations in combination with the scoring functions can overcome the limitations of discriminating between different peptide sequences. This is difficult because the majority of scoring functions have been developed to rank between poses of the same molecules,[71] not different sequences. For the MD simulations, we controlled parameters such as the required sampling time and the potential restrictions applied to the system.[72] We found that using a high temperature (350 K) to sample the binding site is an efficient way to quickly obtain representative conformations. However, to maintain the system stable, it was necessary to restrict the movement of atoms away from the binding region. We found that for peptides that differ approximately in 10 amino acid substitutions, a 100 ns sampling is enough time to have a converged conformational ensemble. As a perspective, one could try single-point mutations to a peptide, after a converged trajectory, and observe how much required sampling time is necessary to obtain a representative equilibrium distribution.[21]

Another crucial aspect is how to score the peptide−MHC class II complexes. First, we found that the inclusion of structural flexibility and the effect of a explicit solvent (through MD simulations) can improve the prediction of binding affinities.[73] This overcomes the limitations commonly found in molecular docking studies, where only a single conformation is used. The analysis over the finite-temperature ensemble showed that several scoring functions had performances with Spearman correlations greater than 0.6. Moreover, we found that such performances can be improved if multiple scoring functions are combined with consensus strategies.[23,74] The fit of a generalized logistic regression model was useful to improve the performances and calculate the weights of the scoring functions. For example, we found that HADDOCK is the scoring function that is less correlated to others functions, and it has assigned one of the biggest weights in both the linear or logistic models. However, we find that the results from the individual scoring functions directly affect the consensus models. In Table 3, we see that peptides SMVGLFSNNPHDLPL and AFALVLLFCALASSC are the ones with poorer individual performance. This poor performance propagates to the consensus model results shown in Table 4. This could be associated with lack of full convergence of the MD simulations (Figure S10).

The proposed protocol can be implemented with other protein−peptide systems and assessed based on the availability of binding data sets. We found in a previous study of nanobody−protein interactions[21] that a similar set of scoring functions predicts rather reliably the binding data. However, it is not guaranteed that the best scoring functions will be the same for all the systems. In such cases, it would be ideal to run a benchmark study as the one described in this work.

Finally, it is important to clarify that our method has a goal similar to sequence-based approaches that rank peptides using binding predictions.[75] However, these sequence-based methods have the limitation that only when the peptides are in the same chemical space used to train the model, the predictions are successful. Moreover, the MHC class II poses larger

DOI: 10.1021/acs.jcim.9b00403
J. Chem. Inf. Model. XXXX, XXX, XXX−XXX

challenges for methods that use training sets because the binding data set is smaller in comparison to the MHC class I.[76] Our approach can overcome such limitations, and provide valuable insights for the *de novo* design of peptides from a computational perspective. Nevertheless, our method requires significant computational resources in comparison to immunoinformatics methods for massive high-throughput predictions. In this case, our approach is suitable for improving known promising peptides through modifications that can be accepted or rejected based on the consensus-scoring strategy.

CONCLUSION

The design of peptides able to bind proteins remains a challenge. Therefore, the development of novel methods for specific complexes, for example MHC class II receptors, is a necessity. In this work, we propose a molecular dynamics-based protocol to rank peptides able to interact with an MHC class II receptor. The integration of MD sampling with different scoring functions allowed to benchmark a set of prediction tools, that in consensus, have the potential to generate average Spearman correlation around 0.8 against available experimental data. Different consensus approaches were tested, and a generalized logistic regression model has the most promising results for further applications. An advantage of our method is the implementation of a rational protocol without involving machine learning approaches, which require large training sets. However, depending on the number of amino acid substitutions between the peptides, the required computational time can increase. In our case, we used 100 ns trajectories for peptides differing in ∼10 amino acids. All-in-all, the modeling, sampling, and scoring strategies are suitable to study and design novel peptides candidates that bind with high affinity to MHC class II, using integrative and consensus strategies.

ASSOCIATED CONTENT

Supporting Information

The Supporting Information is available free of charge on the ACS Publications website at DOI: 10.1021/acs.jcim.9b00403.

Plots monitoring observables from the MD simulations, results of the consensus performances under other configurations and tables with additional data about the scoring functions, as well as descriptions of their methods (PDF)

AUTHOR INFORMATION

Corresponding Author

*P. Cossio. E-mail: pilar.cossio@biophys.mpg.de, grupotandem.biotd@udea.edu.co.

ORCID

Rodrigo Ochoa: 0000-0003-0734-2196

Alessandro Laio: 0000-0001-9164-7907

Pilar Cossio: 0000-0002-5404-9948

Notes

The authors declare no competing financial interest.

ACKNOWLEDGMENTS

The authors thanks Dr. Miguel Soler for his advice about the implementation of some scoring functions, and Dr. Manuel Alfonso Patarroyo and Dr. Carlos Fernando Suarez for their support on the biological insights of the MHC class II system. R.O. and P.C. were supported by Colciencias, University of Antioquia and Ruta N, Colombia, and the Max Planck Society, Germany. The computations were performed in a local server with an NVDIA Titan X GPU. P.C. gratefully acknowledges the support of NVIDIA Corporation for the donation of this GPU.

REFERENCES

(1) Roche, P. A.; Furuta, K. The Ins and Outs of MHC Class II-mediated Antigen Processing and Presentation. *Nat. Rev. Immunol.* **2015**, *15*, 203−216.

(2) Rock, K. L.; Reits, E.; Neefjes, J. Present Yourself! By MHC Class I and MHC Class II Molecules. *Trends Immunol.* **2016**, *37*, 724−737.

(3) Blum, J. S.; Wearsch, P. A.; Cresswell, P. Pathways of Antigen Processing. *Annu. Rev. Immunol.* **2013**, *31*, 443−473.

(4) Bjorkman, P. J. Not Second Class: The First Class II MHC Crystal Structure. *J. Immunol.* **2015**, *194*, 3−4.

(5) Unanue, E. R.; Turk, V.; Neefjes, J. Variations in MHC Class II Antigen Processing and Presentation in Health and Disease. *Annu. Rev. Immunol.* **2016**, *34*, 265−297.

(6) Birnbaum, M. E.; Mendoza, J. L.; Sethi, D. K.; Dong, S.; Glanville, J.; Dobbins, J.; Özkan, E.; Davis, M. M.; Wucherpfennig, K. W.; Garcia, K. C. Deconstructing the Peptide-MHC Specificity of T Cell Recognition. *Cell* **2014**, *157*, 1073−1087.

(7) Knapp, B.; Omasits, U.; Frantal, S.; Schreiner, W. A Critical Cross-Validation of High Throughput Structural Binding Prediction Methods for pMHC. *J. Comput.-Aided Mol. Des.* **2009**, *23*, 301−307.

(8) Neefjes, J.; Jongsma, M. L.; Paul, P.; Bakke, O. Towards a Systems Understanding of MHC Class I and MHC class II Antigen Presentation. *Nat. Rev. Immunol.* **2011**, *11*, 823−836.

(9) Negroni, M. P.; Stern, L. J. The N-terminal Region of Photocleavable Peptides that Bind HLA-DR1 Determines the Kinetics of Fragment Release. *PLoS One* **2018**, *13*, e0199704.

(10) Sewell, A. K. Why Must T Cells be Cross-Reactive? *Nat. Rev. Immunol.* **2012**, *12*, 669−677.

(11) Wang, P.; Sidney, J.; Dow, C.; Mothé, B.; Sette, A.; Peters, B. A Systematic Assessment of MHC Class II Peptide Binding Predictions and Evaluation of a Consensus Approach. *PLoS Comput. Biol.* **2008**, *4*, e1000048.

(12) Nandy, A.; Basak, S. C. A Brief Review of Computer-assisted Approaches to Rational Design of Peptide Vaccines. *Int. J. Mol. Sci.* **2016**, *17*, 666.

(13) Jensen, K. K.; Andreatta, M.; Marcatili, P.; Buus, S.; Greenbaum, J. A.; Yan, Z.; Sette, A.; Peters, B.; Nielsen, M. Improved Methods for Predicting Peptide Binding Affinity to MHC Class II Molecules. *Immunology* **2018**, *154*, 394−406.

(14) Knapp, B.; Omasits, U.; Bohle, B.; Maillere, B.; Ebner, C.; Schreiner, W.; Jahn-Schmid, B. 3-Layer-based Analysis of Peptide-MHC Interaction: In Silico Prediction, Peptide Binding Affinity and T Cell Activation in a Relevant Allergen-Specific Model. *Mol. Immunol.* **2009**, *46*, 1839−1844.

(15) González, R.; Suárez, C. F.; Bohórquez, H. J.; Patarroyo, M. A.; Patarroyo, M. E. Semi-Empirical Quantum Evaluation of Peptide MHC Class II Binding. *Chem. Phys. Lett.* **2017**, *668*, 29−34.

(16) Wieczorek, M.; Abualrous, E. T.; Sticht, J.; Álvaro-Benito, M.; Stolzenberg, S.; Noé, F.; Freund, C. Major Histocompatibility Complex (MHC) Class I and MHC Class II Proteins: Conformational Plasticity in Antigen Presentation. *Front. Immunol.* **2017**, *8*, 1−16.

(17) Wan, S.; Knapp, B.; Wright, D. W.; Deane, C. M.; Coveney, P. V. Rapid, Precise, and Reproducible Prediction of Peptide-MHC Binding Affinities from Molecular Dynamics That Correlate Well with Experiment. *J. Chem. Theory Comput.* **2015**, *11*, 3346−3356.

(18) Wieczorek, M.; Sticht, J.; Stolzenberg, S.; Günther, S.; Wehmeyer, C.; El Habre, Z.; Álvaro-Benito, M.; Noé, F.; Freund, C. MHC Class II Complexes Sample Intermediate States Along the Peptide Exchange Pathway. *Nat. Commun.* **2016**, *7*, 13224.

DOI: 10.1021/acs.jcim.9b00403
J. Chem. Inf. Model. XXXX, XXX, XXX−XXX

(19) Zhang, H.; Wang, P.; Papangelopoulos, N.; Xu, Y.; Sette, A.; Bourne, P. E.; Lund, O.; Ponomarenko, J.; Nielsen, M.; Peters, B. Limitations of Ab Initio Predictions of Peptide Binding to MHC Class II Molecules. *PLoS One* **2010**, *5*, e9272.
(20) Knapp, B.; Demharter, S.; Esmaielbeiki, R.; Deane, C. M. Current Status and Future Challenges in T-Cell Receptor/Peptide/MHC Molecular Dynamics Simulations. *Briefings Bioinf.* **2015**, *16*, 1035−1044.
(21) Soler, M. A.; Fortuna, S.; de Marco, A.; Laio, A. Binding Affinity Prediction of NanobodyProtein Complexes by Scoring of Molecular Dynamics Trajectories. *Phys. Chem. Chem. Phys.* **2018**, *20*, 3438−3444.
(22) Kastritis, P. L.; Bonvin, A. M. Are Scoring Functions in Protein-Protein Docking Ready to Predict Interactomes? Clues From a Novel Binding Affinity Benchmark. *J. Proteome Res.* **2010**, *9*, 2216−2225.
(23) Huang, S.-Y.; Grinter, S. Z.; Zou, X. Scoring Functions and their Evaluation Methods for ProteinLigand Docking: Recent Advances and Future Directions. *Phys. Chem. Chem. Phys.* **2010**, *12*, 12899.
(24) Gladich, I.; Rodriguez, A.; Hong Enriquez, R. P.; Guida, F.; Berti, F.; Laio, A. Designing High-Affinity Peptides for Organic Molecules by Explicit Solvent Molecular Dynamics. *J. Phys. Chem. B* **2015**, *119*, 12963−12969.
(25) Sarti, E.; Gladich, I.; Zamuner, S.; Correia, B. E.; Laio, A. Protein-Protein Structure Prediction by Scoring Molecular Dynamics Trajectories of Putative Poses. *Proteins: Struct., Funct., Bioinf.* **2016**, *84*, 1312−1320.
(26) Ochoa, R.; Watowich, S. J.; Flórez, A.; Mesa, C. V.; Robledo, S. M.; Muskus, C. Drug Search for Leishmaniasis: a Virtual Screening Approach by Grid Computing. *J. Comput.-Aided Mol. Des.* **2016**, *30*, 541−552.
(27) Guida, F.; Battisti, A.; Gladich, I.; Buzzo, M.; Marangon, E.; Giodini, L.; Toffoli, G.; Laio, A.; Berti, F. Peptide Biosensors for Anticancer Drugs: Design In Silico to Work in Denaturizing Environment. *Biosens. Bioelectron.* **2018**, *100*, 298−303.
(28) King, C. A.; Bradley, P. Structure-based Prediction of Protein-Peptide Specificity in Rosetta. *Proteins: Struct., Funct., Bioinf.* **2010**, *78*, 3437−3449.
(29) Obiol-Pardo, C.; Rubio-Martinez, J. Comparative Evaluation of MMPBSA and XSCORE to Compute Binding Free Energy in XIAP-Peptide Complexes. *J. Chem. Inf. Model.* **2007**, *47*, 134−142.
(30) Gromiha, M. M.; Yugandhar, K.; Jemimah, S. ProteinProtein Interactions: Scoring Schemes and Binding Affinity. *Curr. Opin. Struct. Biol.* **2017**, *44*, 31−38.
(31) Moal, I. H.; Torchala, M.; Bates, P. a.; Fernández-Recio, J. The Scoring of Poses in Protein-Protein Docking: Current Capabilities and Future Directions. *BMC Bioinf.* **2013**, *14*, 286.
(32) Wang, P.; Sidney, J.; Kim, Y.; Sette, A.; Lund, O.; Nielsen, M.; Peters, B. Peptide Binding Predictions for HLA DR, DP and DQ Molecules. *BMC Bioinf.* **2010**, *11*, 568.
(33) Vita, R.; Overton, J. A.; Greenbaum, J. A.; Ponomarenko, J.; Clark, J. D.; Cantrell, J. R.; Wheeler, D. K.; Gabbard, J. L.; Hix, D.; Sette, A.; Peters, B. The Immune Epitope Database (IEDB) 3.0. *Nucleic Acids Res.* **2015**, *43*, D405−D412.
(34) Berman, H. M.; Westbrook, J.; Feng, Z.; Gilliland, G.; Bhat, T. N.; Weissig, H.; Shindyalov, I. N.; Bourne, P. E. The Protein Data Bank. *Nucleic Acids Res.* **2000**, *28*, 235−242.
(35) Smith, K. J.; Pyrdol, J.; Gauthier, L.; Wiley, D. C.; Wucherpfennig, K. W. Crystal Structure of HLA-DR2 (DRA*0101, DRB1*1501) Complexed with a Peptide from Human Myelin Basic Protein. *J. Exp. Med.* **1998**, *188*, 1511−20.
(36) Krivov, G. G.; Shapovalov, M. V.; Dunbrack, R. L. Improved Prediction of Protein Side-Chain Conformations with SCWRL4. *Proteins: Struct., Funct., Bioinf.* **2009**, *77*, 778−795.
(37) Rapin, N.; Hoof, I.; Lund, O.; Nielsen, M. MHC Motif Viewer. *Immunogenetics* **2008**, *60*, 759−765.
(38) Andreatta, M.; Karosiene, E.; Rasmussen, M.; Stryhn, A.; Buus, S.; Nielsen, M. Accurate Pan-Specific Prediction of Peptide-MHC Class II Binding Affinity with Improved Binding Core Identification. *Immunogenetics* **2015**, *67*, 641−650.
(39) Loffler, P.; Schmitz, S.; Hupfeld, E.; Sterner, R.; Merkl, R. Rosetta:MSF: a Modular Framework for Multi-state Computational Protein Design. *PLoS Comput. Biol.* **2017**, *13*, e1005600.
(40) Ochoa, R.; Soler, M. A.; Laio, A.; Cossio, P. Assessing the Capability of In Silico Mutation Protocols for Predicting the Finite Temperature Conformation of Amino Acids. *Phys. Chem. Chem. Phys.* **2018**, *20*, 25901−25909.
(41) Huang, P.-S.; Ban, Y.-E. A.; Richter, F.; Andre, I.; Vernon, R.; Schief, W. R.; Baker, D. RosettaRemodel: A Generalized Framework for Flexible Backbone Protein Design. *PLoS One* **2011**, *6*, e24109.
(42) Hess, B.; Kutzner, C.; van der Spoel, D.; Lindahl, E. GROMACS 4: Algorithms for Highly Efficient, Load Balanced, and Scalable Molecular Simulations. *J. Chem. Theory Comput.* **2008**, *4*, 435−447.
(43) Lindorff-Larsen, K.; Piana, S.; Palmo, K.; Maragakis, P.; Klepeis, J. L.; Dror, R. O.; Shaw, D. E. Improved Side-Chain Torsion Potentials for the Amber ff99SB Protein Force Field. *Proteins: Struct., Funct., Bioinf.* **2010**, *78*, 1950−1958.
(44) Jorgensen, W. L.; Chandrasekhar, J.; Madura, J. D.; Impey, R. W.; Klein, M. L. Comparison of Simple Potential Functions for Simulating Liquid Water. *J. Chem. Phys.* **1983**, *79*, 926−935.
(45) Di Pierro, M.; Elber, R.; Leimkuhler, B. A Stochastic Algorithm for the Isobaric-Isothermal Ensemble with Ewald Summations for All Long Range Forces. *J. Chem. Theory Comput.* **2015**, *11*, 5624−5637.
(46) Janežič, D.; Merzel, F. An Efficient Symplectic Integration Algorithm for Molecular Dynamics Simulations. *J. Chem. Inf. Model.* **1995**, *35*, 321−326.
(47) Bussi, G.; Donadio, D.; Parrinello, M. Canonical Sampling Through Velocity Rescaling. *J. Chem. Phys.* **2007**, *126*, 014101.
(48) Parrinello, M.; Rahman, A. Crystal Structure and Pair Potentials: A Molecular Dynamics Study. *Phys. Rev. Lett.* **1980**, *45*, 1196−1199.
(49) Cossio, P.; Laio, A.; Pietrucci, F. Which Similarity Measure is Better for Analyzing Protein Structures in a Molecular Dynamics Trajectory? *Phys. Chem. Chem. Phys.* **2011**, *13*, 10421.
(50) Alford, R. F.; Leaver-Fay, A.; Jeliazkov, J. R.; O'Meara, M. J.; DiMaio, F. P.; Park, H.; Shapovalov, M. V.; Renfrew, P. D.; Mulligan, V. K.; Kappel, K.; Labonte, J. W.; Pacella, M. S.; Bonneau, R.; Bradley, P.; Dunbrack, R. L.; Das, R.; Baker, D.; Kuhlman, B.; Kortemme, T.; Gray, J. J. The Rosetta All-Atom Energy Function for Macromolecular Modeling and Design. *J. Chem. Theory Comput.* **2017**, *13*, 3031−3048.
(51) Krissinel, E.; Henrick, K. Inference of Macromolecular Assemblies from Crystalline State. *J. Mol. Biol.* **2007**, *372*, 774−797.
(52) Andrusier, N.; Nussinov, R.; Wolfson, H. J. FireDock: Fast Interaction Refinement in Molecular Docking. *Proteins: Struct., Funct., Bioinf.* **2007**, *69*, 139−159.
(53) Pierce, B.; Weng, Z. ZRANK: Reranking Protein Docking Predictions with an Optimized Energy Function. *Proteins: Struct., Funct., Bioinf.* **2007**, *67*, 1078−1086.
(54) Cossio, P.; Granata, D.; Laio, A.; Seno, F.; Trovato, A. A Simple and Efficient Statistical Potential for Scoring Ensembles of Protein Structures. *Sci. Rep.* **2012**, *2*, 1−8.
(55) Sarti, E.; Zamuner, S.; Cossio, P.; Laio, A.; Seno, F.; Trovato, A. BACHSCORE. A Tool for Evaluating Efficiently and Reliably the Quality of Large Sets of Protein Structures. *Comput. Phys. Commun.* **2013**, *184*, 2860−2865.
(56) Sarti, E.; Granata, D.; Seno, F.; Trovato, A.; Laio, A. Native Fold and Docking Pose Discrimination by the Same Residue-based Scoring Function. *Proteins: Struct., Funct., Bioinf.* **2015**, *83*, 621−630.
(57) Berrera, M.; Molinari, H.; Fogolari, F. Amino Acid Empirical Contact Energy Definitions for Fold Recognition in the Space of Contact Maps. *BMC Bioinf.* **2003**, *4*, 8.
(58) Fogolari, F.; Corazza, A.; Yarra, V.; Jalaru, A.; Viglino, P.; Esposito, G. Bluues: a Program for the Analysis of the Electrostatic Properties of Proteins Based on Generalized Born Radii. *BMC Bioinf.* **2012**, *13*, S18.

DOI: 10.1021/acs.jcim.9b00403
J. Chem. Inf. Model. XXXX, XXX, XXX−XXX

(59) Dominguez, C.; Boelens, R.; Bonvin, A. M. J. J. HADDOCK: A Protein Protein Docking Approach Based on Biochemical or Biophysical Information. *J. Am. Chem. Soc.* **2003**, *125*, 1731−1737.
(60) Trott, O.; Olson, A. J. AutoDock Vina: Improving the Speed and Accuracy of Docking with a New Scoring Function, Efficient Optimization, and Multithreading. *J. Comput. Chem.* **2009**, *31*, 455−461.
(61) Yang, Y.; Zhou, Y. Specific Interactions for Ab Initio Folding of Protein Terminal Regions with Secondary Structures. *Proteins: Struct., Funct., Bioinf.* **2008**, *72*, 793−803.
(62) Zhou, H.; Skolnick, J. GOAP: A Generalized Orientation-dependent, All-atom Statistical Potential for Protein Structure Prediction. *Biophys. J.* **2011**, *101*, 2043−2052.
(63) Vreven, T.; Hwang, H.; Weng, Z. Integrating Atom-based and Residue-based Scoring Functions for Protein-Protein Docking. *Protein Sci.* **2011**, *20*, 1576−1586.
(64) Fernandez-Recio, J.; Totrov, M.; Skorodumov, C.; Abagyan, R. Optimal Docking Area: A New Method for Predicting Protein-Protein Interaction Sites. *Proteins: Struct., Funct., Bioinf.* **2005**, *58*, 134−143.
(65) Pons, C.; Talavera, D.; De La Cruz, X.; Orozco, M.; Fernandez-Recio, J. Scoring by Intermolecular Pairwise Propensities of Exposed Residues (SIPPER): A New Efficient Potential for Protein-Protein Docking. *J. Chem. Inf. Model.* **2011**, *51*, 370−377.
(66) Xue, L. C.; Rodrigues, J. P.; Kastritis, P. L.; Bonvin, A. M.; Vangone, A. PRODIGY: A Web Server for Predicting the Binding Affinity of Protein-Protein Complexes. *Bioinformatics* **2016**, *32*, 3676−3678.
(67) Pedregosa, F.; Varoquaux, G.; Gramfort, A.; Michel, V.; Thirion, B.; Blondel, M.; Prettenhofer, P.; Weiss, R.; Dubourg, V.; Vanderplas, J.; Passos, A.; Cournapeau, D.; Brucher, M.; Perrrot, M.; Duchesnay, E. Scikit-learn: Machine learning in Python. *J. Mach. Learn. Res.* **2011**, *12*, 2825−2830.
(68) Mansiaux, Y.; Joseph, A. P.; Gelly, J. C.; de Brevern, A. G. Assignment of PolyProline II Conformation and Analysis of Sequence Structure Relationship. *PLoS One* **2011**, *6*, e18401.
(69) Skwarczynski, M.; Toth, I. Peptide-based Synthetic Vaccines. *Chem. Sci.* **2016**, *7*, 842−854.
(70) Meister, D.; Taimoory, S. M.; Trant, J. F. Unnatural Amino Acids Improve Affinity and Modulate Immunogenicity: Developing Peptides to Treat MHC Type II Autoimmune Disorders. *J. Pept. Sci.* **2019**, *111*, e24058.
(71) Li, Y.; Liu, Z.; Li, J.; Han, L.; Liu, J.; Zhao, Z.; Wang, R. Comparative Assessment of Scoring Functions on an Updated Benchmark: 1. Compilation of the Test Set. *J. Chem. Inf. Model.* **2014**, *54*, 1700−1716.
(72) Omasits, U.; Knapp, B.; Neumann, M.; Steinhauser, O.; Stockinger, H.; Kobler, R.; Schreiner, W. Analysis of Key Parameters for Molecular Dynamics of pMHC Molecules. *Mol. Simul.* **2008**, *34*, 781−793.
(73) Spiliotopoulos, D.; Kastritis, P. L.; Melquiond, A. S. J.; Bonvin, A. M. J. J.; Musco, G.; Rocchia, W.; Spitaleri, A. dMM-PBSA: A New HADDOCK Scoring Function for Protein-Peptide Docking. *Front. Mol. Biosci.* **2016**, *3*, 46.
(74) Liu, S.; Fu, R.; Zhou, L.-H.; Chen, S.-P. Application of Consensus Scoring and Principal Component Analysis for Virtual Screening against β-Secretase (BACE-1). *PLoS One* **2012**, *7*, e38086.
(75) Nielsen, M.; Lund, O.; Buus, S.; Lundegaard, C. MHC Class II Epitope Predictive Algorithms. *Immunology* **2010**, *130*, 319−328.
(76) Soria-Guerra, R. E.; Nieto-Gomez, R.; Govea-Alonso, D. O.; Rosales-Mendoza, S. An Overview of Bioinformatics Tools for Epitope Prediction: Implications on Vaccine Development. *J. Biomed. Inf.* **2015**, *53*, 405−414.

DOI: 10.1021/acs.jcim.9b00403
J. Chem. Inf. Model. XXXX, XXX, XXX−XXX